Reconfigurable Silicon Photonics Integrated 16-QAM Modulator Driven by Binary Electronics

Francesco Fresi, Antonio Malacarne, Vito Sorianello, Gianluca Meloni, Philippe Velha, Michele Midrio, Veronica Toccafondo, Stefano Faralli, Marco Romagnoli, and Luca Potì, *Member, IEEE*

***Abstract*—A novel silicon photonics integrated reconfigurable nested Mach–Zehnder interferometer including tunable splitters and four independent phase modulators has been designed and fabricated. The architecture enables the generation of offset-free phase–amplitude constellations such as QPSK and 16-QAM by employing simple binary signals with equal peak-to-peak amplitude. The adoption of tunable splitters introduces novel features such as reconfiguration of the output constellation without modification of the RF waveform settings, as well as compensation for imperfections related to fabrication tolerances. The solution presented in this paper is based on travelling wave MZIs and thermally tunable splitters based on doped rib waveguides heated by Joule effect. The scheme minimizes the complexity of the employed architecture together with one of the driving signals. Numerical analysis has been also conducted to better investigate the system behavior and parameter optimization, evaluating the impact of suboptimum settings that might occur in a real implementation. Experimental results show the generation of QPSK signals up to 28 Gbd and 16-QAM signals up to 20 Gbd with measured bit error rate below the conventional FEC level.**

***Index Terms*—Si integration platform, photonic integrated circuits (PICs), Coherent transmitter.**

I. Introduction

NOWADAYS, photonic integration represents the key technology to reduce the costs (in terms of both capex and opex), the energy consumption and the size of the optical components, thus allowing mass production of cost-effective high-performance photonic integrated circuits (PICs) [1]–[4]. Moreover, integration technologies can increase the stability, reliability and robustness of optical transceivers. Silicon photonics provide significant leverage in design and low-cost fabrication of small foot-print device (smaller than alternative platform such as InP or $LiNbO_3$) [3]. Silicon photonics is also strategic in view of monolithic integration with complementary metal–oxide–semiconductor-based electronics. This way, the shortest possible electric interconnects between electronics and photonics could be allowed, and both bondwires and bondpads, usually detrimental for high speed performance, could be avoided. Recent developments also demonstrated the possibility to include laser sources by exploiting heterogeneous integration [4]. Nowadays, a capacity of 100 Gb/s exploiting Si-based modules with dual-polarization quadrature phase shift keying per channel is almost available for metro-regional applications [5], and optical coherent technology offers enormous advantages with respect to systems based on direct detection [6]. In this scenario, monolithic integration with the electronics is also crucial for mass–volume production of transceivers requiring digital signal processing. Another important aspect for the next-generation optical networks is the spectral efficiency, which can be increased by exploiting more complex modulation formats such as 16-quadrature amplitude modulation (QAM). Several architectures to implement 16-QAM signals have been investigated, as in [7]–[10]. Among these, in a previous work we proposed a solution based on a reconfigurable dual-drive in-phase (I) and quadrature (Q) modulator structure, allowing a 16-QAM signal generation as well as QPSK and others formats [10]. In particular, the proposed structure enables 16-QAM generation by simply driving the modulator with equal-amplitude binary electrical signals, thus avoiding complex electronics for the generation of multiple-level signals [12]. Moreover, the presence of tunable optical splitters in [10] allows energy-efficient offset-free 16-QAM generation and minimize the required phase modulators. In [11], the proposed architecture has been monolithically integrated on a InP platform. However, the high spurious amplitude modulation occurring in p-n junction-based phase modulators limited the capabilities of the circuit so much so that only QPSK modulation was successfully demonstrated.

An equivalent reconfigurable nested Mach–Zehnder interferometer (RN-MZI) architecture is presented in this paper exploiting, for the first time, a silicon-on-insulator (SOI) platform developed through a multi-project wafer run [13]. This work is an extension of [14], demonstrating successful back-to-back coherent transmission of 16-QAM up to 20 Gbd and represents a proof-of-concept of the proposed architecture.

Manuscript received February 1, 2016; accepted February 27, 2016. Date of publication March 10, 2016; date of current version May 9, 2016. This work was supported in part by the EC projects TERABOARD, initiative of the Photonics Public Private Partnership under Grant 688510, IRIS under Grant 619194, and the Scuola Superiore Sant'Anna through the ESPION project.

F. Fresi is with the Interuniversity National Consortium for Telecommunications and Scuola Superiore Sant'Anna, Pisa 56124, Italy (e-mail: francesco.fresi@cnit.it).

A. Malacarne, P. Velha, and S. Faralli are with Scuola Superiore Sant'Anna, Pisa 56124, Italy (e-mail: antonio.malacarne@sssup.it; philippe.velha@gmail.com; sfaralli@sssup.it).

V. Sorianello, G. Meloni, V. Toccafondo, M. Romagnoli, and L. Potì are with the Interuniversity National Consortium for Telecommunications, Pisa 56124, Italy (e-mail: vito.sorianello@cnit.it; gianluca.meloni@cnit.it; v.toccafondo@sssup.it; marco.romagnoli@cnit.it; luca.poti@cnit.it).

M. Midrio is with the Interuniversity National Consortium for Telecommunications, Pisa 56124, Italy, and also with the Università degli Studi di Udine, Udine 33100, Italy (e-mail: michele.midrio@uniud.it).

Color versions of one or more of the figures in this paper are available online at http://ieeexplore.ieee.org.

Digital Object Identifier 10.1109/JSTQE.2016.2538725

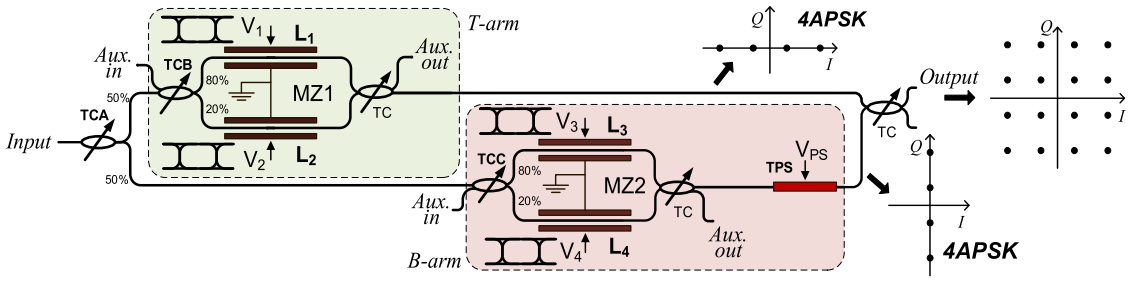

Fig. 1. Scheme of the proposed 16-QAM transmitter with two nested Mach–Zehnder interferometers, including TC and a thermally TPS. The logic diagram for 16-QAM generation as combination of two 4APSK is also shown.

The paper is organized as follows: in Section II the basic concept of the transmitter architecture is presented. Section III is focused on numerical simulations, for investigating on system behavior and the impact of sub-optimum settings that might occur in a real implementation. Section IV describes the PIC design, while Section V reports on experimental results including characterization, testing and a back-to-back transmission experiment with different PIC configurations.

II. Operation Principle

Fig. 1 shows the scheme of the proposed RN-MZI. A detailed description of the operation principle is reported in [11], including numerical analysis to predict the system behavior and discussions about the impact of possible sub-optimum settings in real implementations. The device comprises four phase modulators (L_1, L_2, L_3, L_4) embedded in a double-nested MZI, and tunable optical splitters/couplers (TC). With respect to a conventional dual-drive IQ Mach–Zehnder modulator (MZM), the tunable splitters in the RN-MZI architecture enable the reconfigurability feature: it should be noted that, although in this implementation all splitters/couplers are implemented as TCs, this is not strictly required, as reconfigurability requires only splitters TCA, TCB and TCC to be tunable. Adopting proper splitting ratios, the modulator can easily map (up to four) binary tributaries onto QPSK, four-level optical amplitude and phase shift keying (4APSK), 16-QAM or even more exotic constellation such as hexagonal 16-QAM [10]. Generation of 16-QAM can be achieved by simply driving the modulator with four electrical binary signals with equal peak-to-peak amplitude. In a first configuration (see Fig. 1), a 16-QAM generation is obtained as a combination of two 4APSK signals. To this aim, splitter TCA is kept balanced at 50/50, while splitters TCB and TCC are set to a power splitting ratio equal to 80/20, corresponding to an amplitude ratio of 2. In the top arm (T-arm, MZ1), a 4APSK constellation is produced, corresponding to the in-phase component of the target 16-QAM constellation. MZ1 can be biased either at a maximum (referred to as *in-phase biasing* condition) or a minimum (*out-of-phase biasing*) of its transfer function. More details on this are provided in Section III of this paper and in our previous work [11]. In the same way, in the bottom arm (B-arm) MZ2 provides a second 4APSK, corresponding to the quadrature component. A thermally tunable phase-shifter (TPS) is used to adjust the relative phase between T-arm and B-arm. In order to prevent any residual offset in the final 16-QAM constellation, both the 4APSK constellations generated in the MZ1 and in the MZ2 should be symmetric with respect to the origin of the complex plane. This is obtained by setting the peak-to-peak voltage V_{pp} of the driving binary signals equal to the half wave voltage V_π of each of the four phase modulators.

TABLE I
Tunable Splitters and Bias Configuration for 16-QAM Generation as Combination of 2× 4APSK or 2× QPSK Signals

	2× 4APSK	2× QPSK
Splitter TCA	50/50	80/20
Splitter TCB	80/20	50/50
Splitter TCC	80/20	50/50
MZ1 bias	$\{0, \pi\}$	$\pm\pi/2$
MZ2 bias	$\{0, \pi\}$	$\pm\pi/2$
TPS relative bias	$\pm\pi/2$	$\{0, \pm\pi/2, \pi\}$

In an alternative configuration, shown in Fig. 2, a 16-QAM constellation is obtained as a combination of two QPSK signals with different amplitudes, generated in the two arms respectively, yet requiring only binary driving electronics with the same V_{pp} as in the previous case. To this aim, splitter TCA is set to 80/20 splitting ratio while splitters TCB and TCC are set to a balanced ratio 50/50. DC bias voltages are also modified to set both the two arms into quadrature configuration. Table I summarizes tunable splitters and biases values for the two different configurations.

III. Numerical Simulations

A numerical model of the proposed architecture has been implemented in MATLAB environment. The simulation tool allows to independently vary the power splitting ratios of each input splitter, to set dc biases, peak-to-peak voltage for the RF driving signals as well as the half wave voltage V_π for the phase modulators and the TPS. The tool also takes into account for additional spurious amplitude modulation occurring along the phase modulators. In [11] the model was exploited to investigate in details the potential and critical aspects of the RN-MZI, analyzing the behavior of the system when deviating some parameter from the ideal values. In particular that analysis focused on the deviation of driving signals' peak-to-peak voltage V_{pp} from V_π, the impact of splitting ratio inaccuracy and spurious amplitude modulation along the phase modulators: in the case V_{pp} deviates from V_π, the resulting phase shift is not

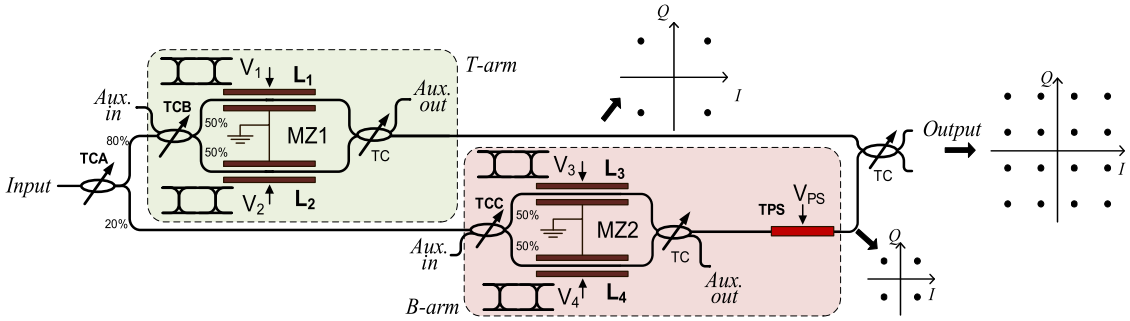

Fig. 2. Scheme of the proposed 16-QAM transmitter when operating in 2× QPSK configuration.

sufficient enough to rotate the four phasors as desired and this induces a residual offset in the constellation. Optical splitters set the amplitude of the interfering fields within the modulator; therefore, splitting ratio inaccuracy affects the symbol distance, resulting into an inhomogeneous distance among different symbols inside the constellation, leading to performance worsening. In addition, spurious amplitude modulation may occur in phase modulators [2]; this means that the optical phasors, while rotating over the complex plane according to the applied signals, are affected by amplitude variation too. This may lead to the presence of an offset in the constellation and unequally spaced constellation symbols that might be partially mitigated through a further tuning of the power splitters.

When all parameters are optimized, the modulator is able to generate an offset free 16-QAM constellation. Furthermore, it is worth discussing about transitions between consecutive symbols too. Despite 16-QAM symbols are symmetric with respect to the origin of the complex plane and the resulting constellation is offset free, transitions might not be symmetric, therefore resulting in a residual offset in the temporal waveform, that might impact on its energy efficiency. Transitions depend on both temporal pulse response and DC biases, that determine how contributions from the four independent phase modulators are combined together. Fig. 3(a) shows transitions when QPSK is generated in one arm of the modulator. Fig. 3(b) and (c) are referred to generation of 4APSK: the inner dual-drive MZM (e.g., MZ1) can be biased either at a maximum (Fig. 3(b), *in-phase biasing*) or a minimum (see Fig. 3(c), *out-of-phase biasing*) of its transfer function. When in-phase biasing is chosen, larger transitions occur with respect to out-of-phase biasing, thus causing a waste of energy. Observing the complete 16-QAM constellation including transitions, it is clear that in-phase biasing (see Fig. 3(d)) results in large asymmetry and high transition peaks. This implies a residual offset in the temporal waveform that causes a waste of energy, thus reducing energy efficiency. On the contrary, out-of-phase biasing (see Fig. 3(e)) exhibits much higher symmetry and lower transition peaks and is therefore more suitable for implementation. It should be noted that these same transitions can be obtained also when 16-QAM is generated as a combination of two QPSK, provided that the relative phase is properly chosen: even though any multiple of $\pi/2$ leads to 16-QAM constellation, only one (out of four possible values) minimizes transitions.

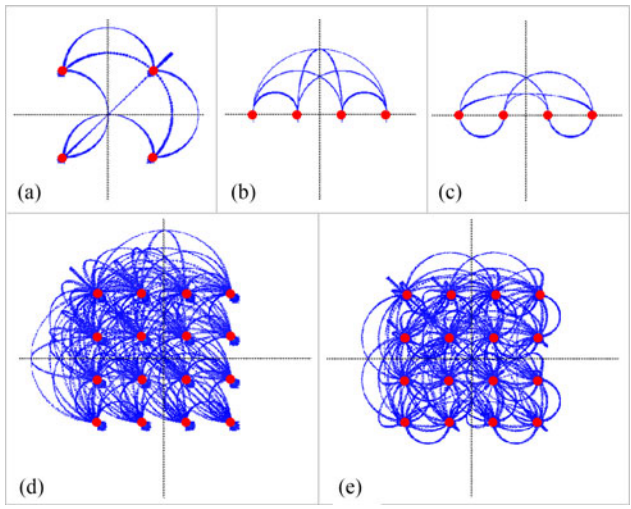

Fig. 3. Numerical simulations showing transitions for different modulator settings: (a) QPSK generation through pure phase modulation in MZ1; (b) generation of 4APSK in case of in-phase biasing; (c) generation of 4APSK in case of out-of-phase biasing; (d) generation of 16-QAM in case of in-phase biasing; (e) generation of 16-QAM in case of out-of-phase biasing.

IV. Photonic Integration Design

The design of the integrated RN-MZI was based on the process flow and the design rules provided by the selected Si photonic platform. In particular, a multi-project wafer run on a standard 220 nm thick SOI platform provided by CMC-IME was chosen [13]. The PIC was designed for single TE polarization with input output coupling obtained through single-polarization grating couplers [15]. The main building blocks of the proposed PIC are the tunable splitters and the MZI modulators. Fig. 4 shows the RN-MZI circuit layout and a picture of a fabricated sample.

A. Tunable Splitter

The splitter was designed in order to achieve a continuous tunability of the power splitting ratio from 0% to 50% in order to allow the full re-configuration of the PIC. The tunable splitter was made of a balanced MZI provided with TPS on each arm and 50/50 directional couplers at the input and output. Fig. 5 shows the tunable coupler scheme (a) and the cross sections of the directional coupler (b) and the designed TPS (c). The 50/50

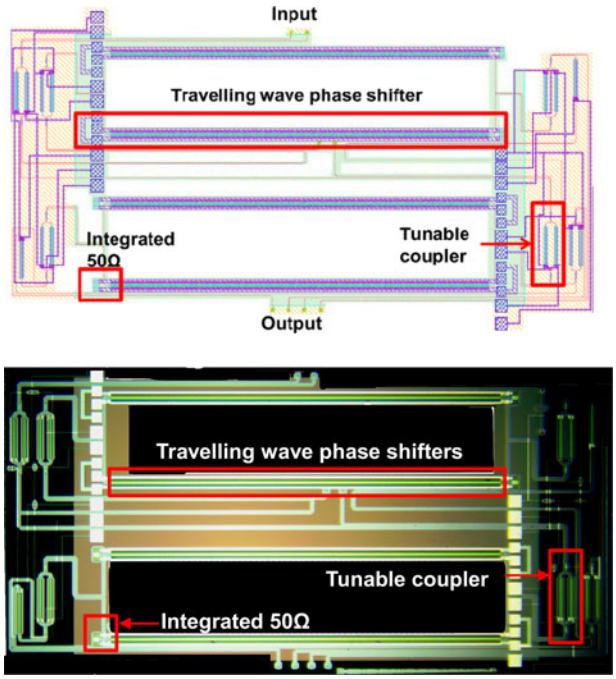

Fig. 4. RN-MZI circuit layout (top) and a picture of a fabricated sample (bottom).

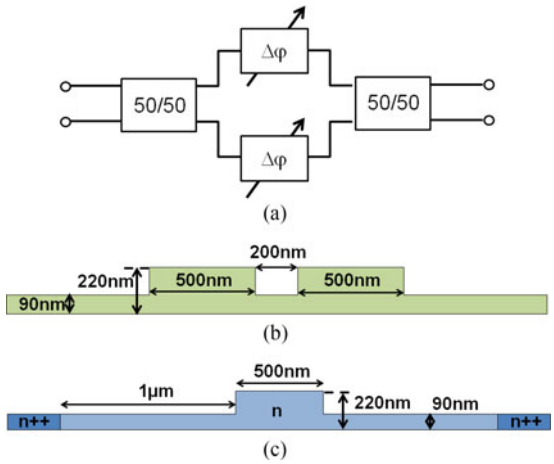

Fig. 5. (a) Tunable coupler schematic. (b) Directional coupler cross section. (c) Thermal phase shifter cross section.

directional coupler is based on rib waveguides with 500 nm wide core and 90 nm thick slab separated by a 200 nm gap (see Fig. 5(b)). Finite element method (FEM) as well as 3-D finite difference time domain (FDTD) simulations were performed in order to determine the proper length of the device, accounting for the contribution of the input and output bends. Fig. 6 shows a top view of the beam propagation at 1550 nm as calculated by the FDTD when the coupling ratio is 50% (a) and the evaluated power coupling ratio at 1550 nm as a function of the straight section length (b). Fig. 6(b) shows the FDTD results for four different straight section length (black circles). The FDTD results were fitted according to the relation [16]:

$$k = \sin\left(\frac{\pi}{2L_x}(x + x_{\text{bend}})\right)^2 \tag{1}$$

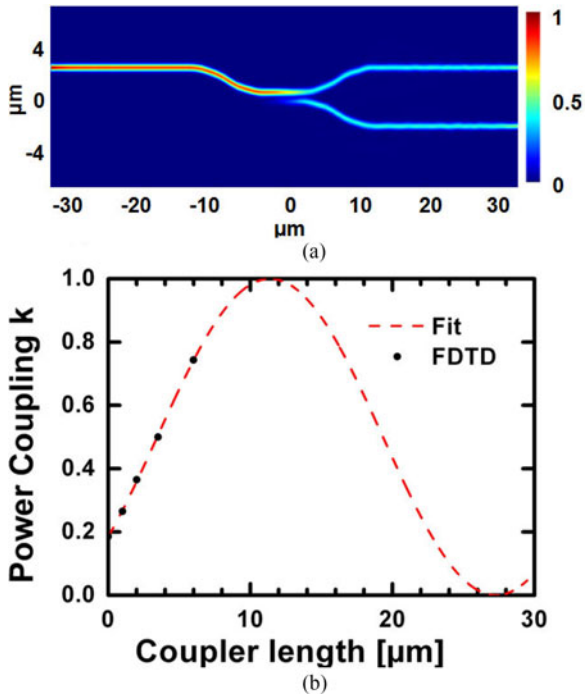

Fig. 6. (a) Top view of the beam propagation at 1550 nm (FDTD). (b) Power coupling ratio at 1550 nm as a function of the straight section length.

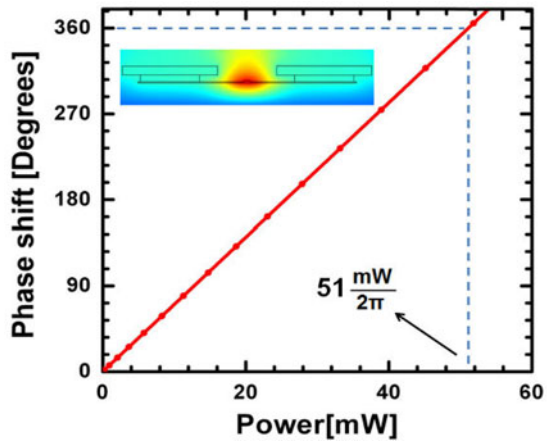

Fig. 7. TPS phase shift versus dissipated power at 1550 nm. In the inset it is shown a qualitative distribution of the temperature when the waveguide is heated up.

where k is the power coupling, L_x is the cross-over length and x_{bend} is the equivalent coupler length due to the access bends when the straight section is 0 μm. From the fit a 50/50 coupling at 1550 nm is derived for a straight section of 3.75 μm.

The TPS (see Fig. 5(c)) consist of a 300 μm straight rib waveguide that is lightly n-type doped. Lateral metal contacts allow the injection of an electric current. From an electrical perspective the device is a resistance heated up by Joule effect. Extensive thermal simulations were performed with an FEM commercial software in order to determine the phase shifter efficiency. Fig. 7 shows the expected phase shift versus dissipated power at 1550 nm wavelength. In the proposed configuration the

current flows right through the waveguide and the Joule effect occurs at the center of the waveguide, see the inset of Fig. 7, maximizing the thermo-optic effect. The designed phase shifter is 300 μm long with an expected efficiency of 51 mW for a 2π phase shift.

B. MZI Modulator

The RN-MZI core consists of two travelling wave MZIs (TWMZI). Each TWMZI is a balanced MZI where each RF arm is a segmented 3 mm long p-n junction rib waveguide driven by an Aluminum (Al) transmission line (TL). The modulator design involved two main studies. The first part of the design was dedicated to the definition of the waveguide cross section in terms of geometry and doping in order to optimize the modulation efficiency and bandwidth. The second task was dedicated to the segmented TL with two main objectives: the matching of the RF and optical mode velocities, and the achievement of an equivalent impedance of 50 Ω for the TL loaded with the p-n junction.

The p-n junction was studied by TCAD simulations in order to determine the junction capacitance and optimize the series resistance per unit length complying with the available process design rules. With the available doping, a junction capacitance lower than 1.6 pF/cm was estimated for reverse bias larger than 1 V and a series resistance as low as 1 Ω·cm.

The waveguide properties at different electrical biases were studied with a commercial mode solver integrating free carriers simulations in order to assess the insertion loss and modulation efficiency. An average insertion loss per arm of 6 dB was estimated as well as a $V_\pi L$ product of 2.2 V·cm. From this simulation an optical group index of 3.9 was evaluated.

The group index should be matched by the loaded TL effective index in order to match the RF and optical mode velocities. In particular, as the RF mode is largely faster than the optical one, the p-n junction capacitance is used to load the TL and slow down the RF mode [17]. A commercial FEM software was used to evaluate the effective index and impedance of the TL without load and to be used with the results of the TCAD simulations in order to determine the equivalent effective index and impedance of the loaded TL. Optimizing the TL geometry the waveguide optical effective index and the 50 Ω impedance target were matched at the same time. Fig. 8 shows the cross section of the designed TL (a), the equivalent impedance and effective index versus frequency of the TL loaded with the p-n junction waveguide (b). Both the effective index and the equivalent impedance are fully matched with the desired value of 3.9 and 50 Ω, respectively. In the fabricated device termination load of 50 Ω has been integrated on the PIC. In particular, the 50 Ω termination consists of a doped Si area electrically connected at the end of the TL. Finally Fig. 9 shows the electro-optic bandwidth of the segmented TWMZI, calculated at different biases [17]. The designed modulator exhibit an electro-optical 3 dB bandwidth of 22 GHz for a matched impedance of 50 Ω when the p-n junction is biased at 0 V. The bandwidth rapidly increases up to 33 GHz for reverse biases larger than 2 V because of the p-n junction capacitance reduction.

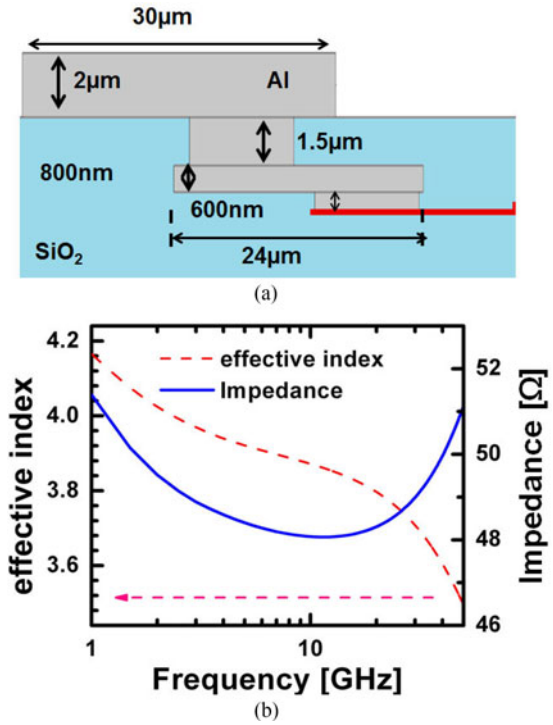

Fig. 8. (a) Cross section of the TL (left arm). (b) Effective index and equivalent impedance of the TL loaded with the p-n junction waveguide.

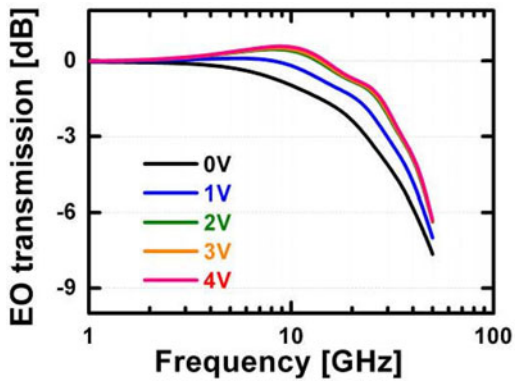

Fig. 9. Simulated electro-optic bandwidth of the segmented TWMZI modulator at different reverse bias.

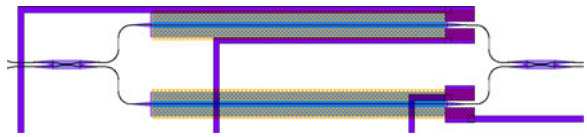

Fig. 10. Mask layout of a tunable splitter/coupler which consists of a balanced Mach–Zehnder interferometer with integrated heaters on each branch.

V. Experimental Results

A. PIC Characterization

Each building block has been characterized beforehand in order to assess the performances of the modulator. Fig. 10 shows the mask layout of the tunable splitter/coupler, realized through a balanced MZI encompassing two 50/50 directional couplers

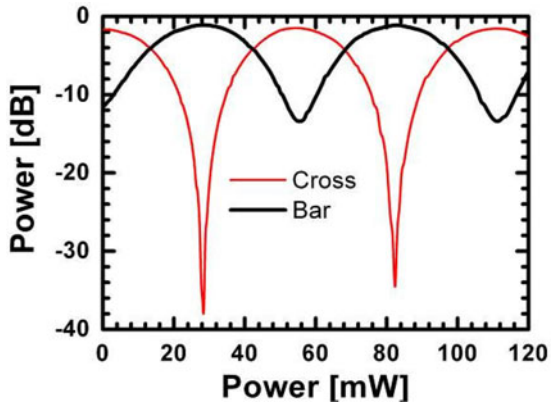

Fig. 11. Characteristic of the tunable coupler as a function of the electrical power injected in one of the heaters for the cross and bar port.

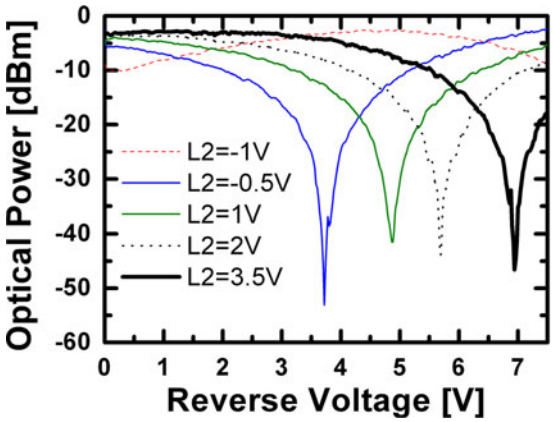

Fig. 12. Optical transfer function of MZ1 as a function of the reverse bias of L_1 for different values of Bias on L_2.

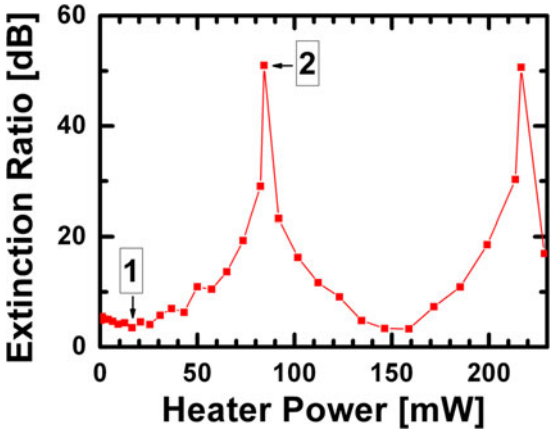

Fig. 13. ER of the modulator as a function of the electrical power given to one of the tunable couplers.

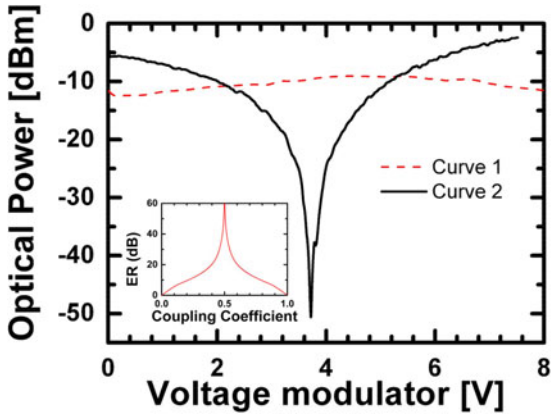

Fig. 14. Optical transfer function of Mach–Zehnder (MZ1) as a function of the reverse voltage on the phase modulator L_2 for 2 condition of the tunable coupler (point 1 and 2 of Fig. 13). In inset, modeled ER in dB as a function of the coupler splitting ration of the Mach–Zehnder.

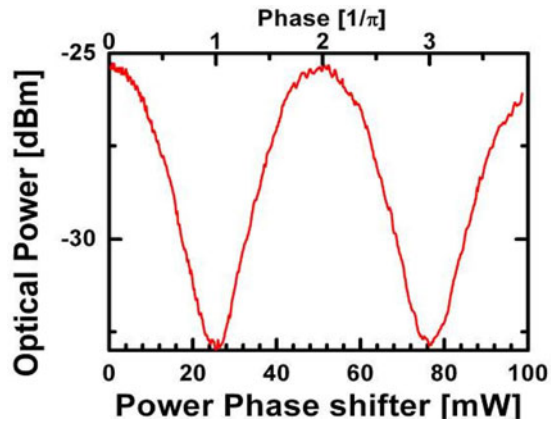

Fig. 15. Optical Transfer function of the nested MZI as a function of the phase shift given by the TPS.

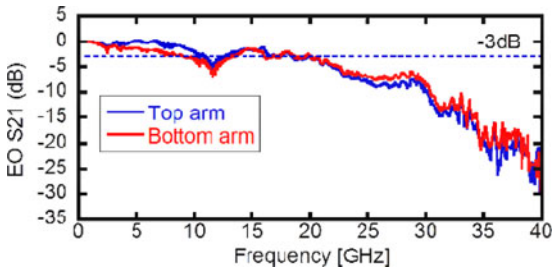

Fig. 16. Experimental optoelectronic S21 transmission of the TWMZI modulator.

and TPSs, as detailed in Section IV-A. Any change of the waveguide refractive index in any of the two arms, induced by heating of the TPS through injection of an electric current, unbalances the MZI and therefore changes the phase condition at the output directional coupler. In Fig. 11 is shown the optical transfer function of the TC coupler as a function of the electrical power injected in one of the heaters for the Cross and Bar port. The coupling coefficient can be tuned from less than 10% up to over 90%. The switching efficiency is around 55 mW/FSR (free spectral range).

The TWMZIs have been characterized measuring the optical transfer function. As expected from the depletion mechanism, the losses of the modulator over a full FSR are negligible (<3 dB). V_π around 4.6 V was measured evaluating the optical

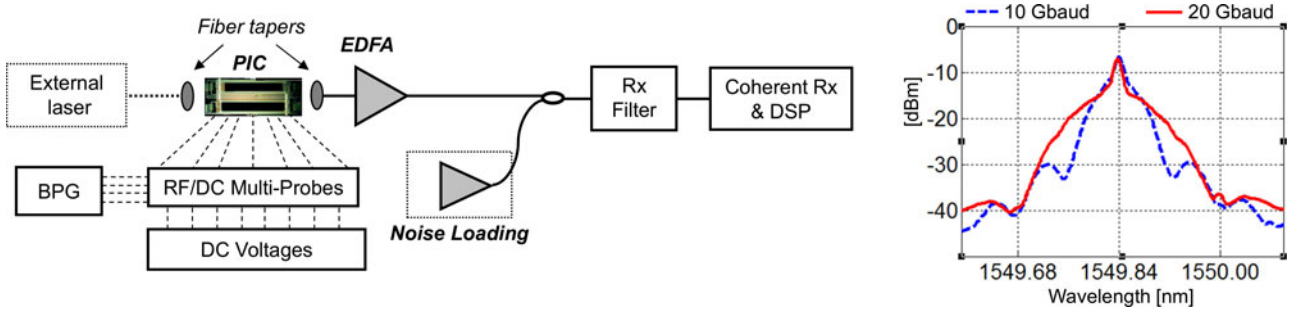

Fig. 17. Experimental set-up (left) and optical spectra of the generated 16-QAM signals (right).

transfer function of MZ1 as a function of the reverse bias of L_1 for different values of Bias on L_2, as shown in Fig. 12.

Furthermore, as shown in Fig. 13, by properly adjusting the TC splitting ratio it is possible to arbitrarily control the coupling coefficient (balance) of the MZI, ranging from nominal 0/100 (point 1) till 50/50 (point 2), enabling a "dazzling" extinction ratio (ER) in excess of 50 dB. In Fig. 14 are reported the curves corresponding to the two opposite cases of totally unbalanced MZI (dashed), or perfectly balanced MZI (solid), corresponding to points 1 and 2 in Fig. 13, respectively. It should also be noted that no significant spurious amplitude modulation occurs along the phase modulators, and this is of particular importance to achieve pure phase modulation in each TL. The inset in Fig. 14 reports the modelled ER of a MZI as a function of the input coupler ratio, showing very good matching with Fig. 13.

Finally, in Fig. 15 is reported the optical transfer function of the whole RN-MZI as a function of the phase shift given by the TPS. In this case the efficiency is 54 mW/2π and the characteristic does not exhibit any losses.

In order to evaluate the RF performances of the phase modulators Fig. 16 shows the experimental optoelectronic S21 transmission magnitude of the two arms of one of the fabricated TWMZI modulators, revealing an experimental 3 dB bandwidth of about 20 GHz at the operating bias of 5 V. The measured bandwidth is lower than expected. This is due to thermal effects at the integrated resistive load. In particular, the large bias induces a local heating of the Si resistance which increases significantly preventing the correct impedance matching with the TL. A future improvement of this impairment is the integration of a dc block on chip in order to avoid the resistance heating. A static $V_\pi L$ product of about 2.4 V·cm is estimated which corresponds for the case of a 3 mm long phase modulator to about 7 $V_{\rm pp}$ for a $\pi/2$ phase shift as required by the 16-QAM modulation conditions.

B. QPSK Modulation Experiment

After characterization of the main building blocks, a transmission experiment in back-to-back with self-homodyne coherent detection has been set up as shown in Fig. 17. All the electrical bias and RF signals are provided to the whole structure by means of two multi-contact wedge probes provided with two RF ground–signal–ground and seven dc probes each. Light is coupled into and collected out of the chip and through single mode

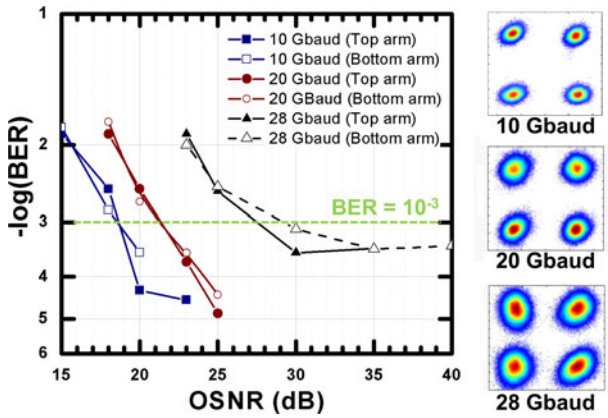

Fig. 18 BER measurements versus OSNR for QPSK generation in both top arm (MZ1) and bottom arm (MZ2), for symbol rate up to 28 Gbd. Recovered constellations are shown on the right.

fibers through the grating couplers, which exhibit an insertion loss of about 5 dB each. An external cavity laser (linewidth = 150 kHz) is used as optical carrier and fed to the transmitter PIC through the input port. Preliminary measurements have been conducted demonstrating QPSK generation in one single arm of the nested modulator. In this configuration, only half of the whole structure (MZ1) is exploited, splitter TCA is totally unbalanced towards the T-arm, while splitter TCB is set to balanced 50/50 ratio. The RF input pads of the two phase modulators L_1 and L_2 of MZ1 are driven by two independent binary data streams with same $V_{\rm pp}$ (7 V after RF amplification), provided by a bit pattern generator (BPG). Proper dc voltages are coupled through high frequency bias tees for optimum biasing of the TWMZIs. The relative bias difference is optimized to impose $\pi/2$ relative phase to compose the QPSK constellation. The generated signal is received exploiting coherent detection as in [11], measuring bit error rate (BER). Noise loading has been applied to evaluate performance under different OSNR conditions, and generation and detection of QPSK signal with BER $< 10^{-3}$ has been demonstrated up to 28 Gbd in both T-arm (MZ1) and the B-arm (MZ2). BER measurements are reported in Fig. 18, together with recovered constellations, for symbol rate up to 28 Gbd. Error floor appears for the 28 Gbd case, and was attributed different factors. The first is that at the operating biases the impedance is not correctly matched because of the thermal effect discussed in the previous section. The second is

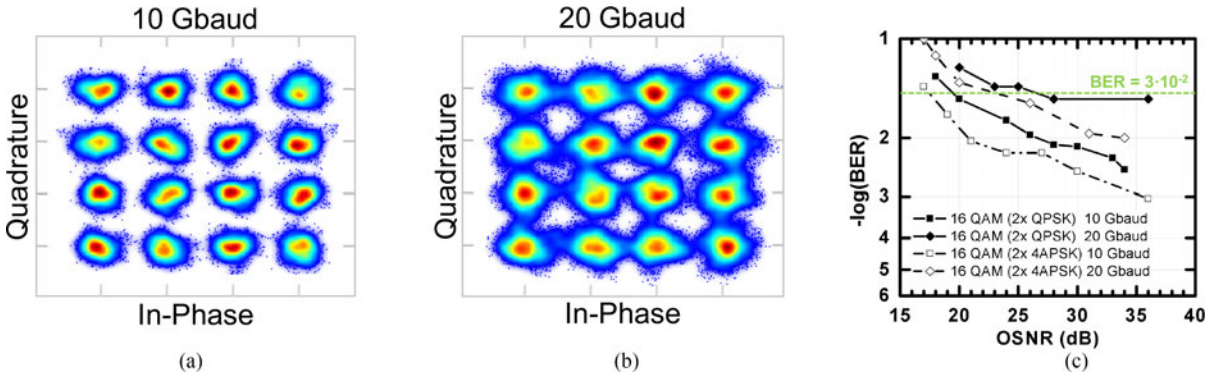

Fig. 19. Recovered constellations of the generated 16-QAM signals at (a) 10 Gbd and (b) 20 Gbd. (c) BER measurements.

due to possible electrical mismatches in the experimental RF routing to the PIC. In these conditions electrical RF reflections may induce the observed floor.

C. 16QAM Modulation

After successful demonstration of QPSK generation in the two arms, 16-QAM operation has been addressed. Four independent binary data streams having all the same $V_{\rm pp}$ (7 V after RF amplification) have been applied to the four RF input pads of the four phase modulators. First, 16-QAM has been obtained as combination of two QPSK signals, as described in Section II and shown in Fig. 2, by setting splitter TCA to 80/20 ratio and splitters TCB and TCC to balanced 50/50. Again, the generated signal is received exploiting coherent detection, evaluating BER as function of the OSNR at the receiver. As reference, we consider state-of-the-art systems employing soft-decision forward error correction, with overhead in the range 7–25%, enabling pre-FEC BER threshold up to $3.4 \cdot 10^{-2}$ or even higher [18]. Performances have been successfully evaluated up to 20 Gbd, and are reported in Fig. 19(c). However, in this configuration the modulator exhibits unstable behavior and is sensitive to environment condition, showing an error floor. Then, the modulator was reconfigured, such that 16-QAM is realized as combination of two orthogonal 4APSK signals, as shown in the operation principle scheme in Fig. 1. Reconfiguration is easily achieved by simply operating on tunable splitters and dc biases. Splitter TCA is set to symmetric 50/50 power ratio while splitters TCB and TCC are unbalanced to 80/20. DC biases in MZ1 and MZ2 are set to out-of-phase condition (see Section II), while $\pi/2$ relative phase is imposed between T-arm and B-arm by changing the injected current in the TPS. This configuration appeared more stable and allowed improved performance, as reported in Fig. 19. Correct generation of a 16-QAM constellation is demonstrated for symbol rate up to 20 Gbd. The optical spectra and recovered constellations are reported in Figs. 17 and 19, respectively.

These results confirm the effectiveness of the proposed scheme and bring a significant improvement with respect to results obtained with InP implementation [11]. Nevertheless, it is worth discussing about the performance gap experienced between the two different configurations. In principle, same performance would be expected when generating 16-QAM through combination of two QPSK or, alternatively, two 4APSK. As mentioned in Sections II and III, both configurations may lead to offset free constellations and same transitions between symbols. However, in our experimental implementation, the sample PIC appeared to be more suitable for implementing the latter. This is motivated by a higher required current to be injected in the thermally-controlled tunable splitters for the QPSK-based configuration. With respect to the 4APSK-based configuration, this resulted in a less stable temperature control of the PIC.

VI. Conclusion

A novel Silicon integrated reconfigurable double nested Mach–Zehnder interferometer has been designed, fabricated and characterized. This novel PIC is based on a single IQ modulator structure including optical power splitters with tunable splitting ratio and four independent phase modulators driven by four equal-amplitude binary signals. Each thermally tunable splitter consists of a balanced MZI with thermal phase shifters based on doped rib waveguides heated by Joule effect, while the modulator core is based on two travelling wave with RF arms consisting of segmented 3 mm long p-n junction rib waveguide driven by an Al TL.

The transmitter architecture enables mapping of up to four independent electrical binary data streams onto offset-free reconfigurable output constellations (QPSK, 4APSK, 16-QAM). Furthermore, fine tuning of the mentioned splitting ratios also enables compensation for imperfections related to the fabrication. Generation of optical 16-QAM exploiting only binary electronic driving signals has been successfully demonstrated up to 20 Gbd. Reconfigurability features have been proved, demonstrating 16-QAM generation either as combination of two QPSK signals or by combining two 4APSK. Furthermore, QPSK operation up to 28 Gbd has been demonstrated exploiting pure phase modulation into one half of the structure, employed as a dual-drive MZM.

This solution introduces reconfigurability features and brings advantages with respect to conventional 16-QAM schemes, that typically produce either a constellation with an offset, or make use of more complex architectures, or they are driven by multiple-level signals or by binary signals with different amplitudes.

ACKNOWLEDGMENT

The authors would like to thank the NSERC SiEPIC Program for training and component library, and CMC Microsystems for the foundry service and fruitful technical discussions.

REFERENCES

[1] A. Malik, T. Neel, O. Turkcu, S. Hand, and S. Melle, "Photonic integration—Path towards energy efficient optical transport networks," in *Proc. IEEE Int. Conf. Adv. Netw. Telecommun. Syst.*, Dec. 14–17, 2014, pp. 1–3.

[2] C. R. Doerr, "Silicon photonic integration in telecommunications," *Front. Phys.*, vol. 3, no. 37, 2015, doi: 10.3389/fphy.2015.00037.

[3] D. Liang and J. E. Bowers, "Photonic integration: Si or InP substrates?" *Electron. Lett.*, vol. 45, no. 12, pp. 578–581, Jun. 4, 2009.

[4] G. Roelkens *et al.*, "III-V-on-silicon photonic devices for optical communication and sensing," *Photon. Multidisciplinary Digital Publishing Inst.*, vol. 2, no. 3, pp. 969–1004, 2015.

[5] T. N. Nielsen *et al.*, "Engineering silicon photonics solutions for metro DWDM," presented at the *Optical Fiber Communications Conf. Exhibition*, San Francisco, CA, USA, Mar. 9–13, 2014, Paper Th3J.1.

[6] G. Bennett *et al.*, "A review of high-speed coherent transmission technologies for long-haul DWDM transmission at 100 g and beyond," *IEEE Commun. Mag.*, vol. 52, no. 10, pp. 102–110, Oct. 2014.

[7] A. H. Gnauck *et al.*, "Spectrally efficient long-haul WDM transmission using 224-Gb/s polarization-multiplexed 16-QAM," *J. Lightw. Technol.*, vol. 29, no. 4, pp. 373–377, Feb. 15, 2011.

[8] X. Zhou and J. Yu, "200-Gb/s PDM-16QAM generation using a new synthesizing method," presented at the *Eur. Conf. Optical. Communication.*, Vienna, Austria, Sep. 20–24, 2009.

[9] S. Yan *et al.*, "Generation of square or hexagonal 16-qam signals using a single dual drive IQ modulator driven by binary signals," in *Proc. Opt. Fiber Commun. Conf.*, 2012, pp. 1–3.

[10] A. Malacarne *et al.*, "Versatile offset-free 16-QAM single dual-drive IQ modulator driven by binary signals," *Opt. Lett.*, vol. 37, pp. 4149–4151, 2012.

[11] F. Fresi *et al.*, "Integrated reconfigurable coherent transmitter driven by binary signals," *IEEE J. Sel. Topics Quantum Electron.*, vol. 21, no. 6, pp. 1–10, Nov./Dec. 2015.

[12] N. Kikuchi, "Intersymbol interference (ISI) suppression technique for optical binary and multilevel signal generation," *J. Lightw. Technol.*, vol. 25, no. 8, pp. 2060–2068, Aug. 2007.

[13] [Online]. Available: http://www.cmc.ca/en/WhatWeOffer/Photonics.aspx

[14] F. Fresi *et al.*, "Silicon photonics integrated 16-qam modulator exploiting only binary driving electronics," presented at the *Optical Fiber Communications Conf. Exhibition*, Anaheim, CA, USA, Mar. 20–24, 2016, Paper Th3J.6.

[15] Y. Wang *et al.*, "Universal grating coupler design," *Proc. SPIE Photon. North*, vol. 8915, pp. 89150Y–1–89150Y-7, 2013.

[16] L. Chrostowsky *et al.*, *Silicon Photonics Design*. Cambridge, U.K.: Cambridge Univ. Press, Feb. 2015.

[17] G. L. Li *et al.*, "Analysis of segmented traveling-wave optical modulators," *J. Lightw. Technol.*, vol. 22, no. 7, pp. 1789–1796, Jul. 2004.

[18] T. Rahman *et al.*, "Ultralong Haul 1.28-Tb/s PM-16QAM WDM transmission employing hybrid amplification," *J. Lightw. Technol.*, vol. 33, no. 9, pp. 1794–1804, May 1, 2015.

Francesco Fresi received the M.S. degree in telecommunications engineering from the University of Pisa, Pisa, Italy, in 2005, and the Ph.D. degree from Scuola Superiore Sant'Anna, Pisa, in 2009. In 2009, he received a short-term scholarship as a Visiting Student from the Institut National de la Recherche Scientifique, Montreal, QC, Canada, in the Ultrafast Optical Processing Group. He was an Assistant Professor with Scuola Superiore Sant'Anna from 2010 to 2015. He is currently an Affiliate Researcher at the National Laboratory for Photonic Networks of National Interuniversity Consortium for Telecommunications, Pisa, in the high-capacity optical communications area. His research interests include the area of fiber optic communications, with particular interest in high-capacity coherent optical communication with high spectral efficiency photonic integrated transceivers and elastic networking. He is (co-)author of more than 30 publications in international journals and more than 50 conference proceedings, and patents.

Antonio Malacarne received the Ph.D. degree in ICT (telecommunication area) from Scuola Superiore Sant'Anna (SSSA), Pisa, Italy, in 2009. He is currently a Research Fellow at the Institute of Communication, Information and Perception Technologies, SSSA, in the areas "high-capacity optical communications" and "digital and microwave technologies." His career includes a two-year long postdoctoral position at the National Institute of Scientific Research, Montreal, QC, Canada, with Prof. J. Azaña. He is currently involved in numerous European/International/National projects including the EU project RAPIdO (FP7-ICT-2013-11), where he is an STC Member. He is an author of 28 manuscripts published in international journals, more than 60 contributions for international conferences, and five international patents. His research interests include integrated optical transceivers, optical interconnects, photonic processing, and microwave photonics.

Vito Sorianello received the Ph.D. degree in electronic engineering from Roma Tre University, Rome, Italy, in 2010. In 2010, he received the IEEE Best Doctoral Thesis Award for his Ph.D. thesis on "Germanium-on-Silicon near-infrared photodetectors" by the IEEE Photonics Society Italian Chapter. He was a Postdoctoral Research Fellow with the Nonlinear Optics and OptoElectronics Lab of Roma Tre University, being involved and responsible for the fabrication and characterization processes of Germanium-on-Silicon photodetectors for three years. He has been a Researcher at the Photonic Networks National Lab, Interuniversity National Consortium for Telecommunications, Pisa, since 2013. His main research interests include the modeling, design, and characterization of optoelectronic components and systems for the silicon photonics platform. He is currently involved in several application-oriented research projects in collaboration with national and international research institutions and industries.

Gianluca Meloni received the Laurea degree in telecomunications engineering from the University of Pisa, Pisa, Italy, in 2003, and the Ph.D. degree from Scuola Superiore Sant'Anna (SSSA), Pisa, in 2008. He was a Visiting Student with the Optoelectronics Research Centre, University of Southampton, Southampton, U.K. He is currently an Executive Research Technician at the National Interuniversity Consortium for Telecommunications in the high-capacity optical communications area and an Affiliate Researcher at the Institute of Communication, Information and Perception Technologies, SSSA. He is a coauthor of 3 book chapters, more than 25 papers on international journals, 40 invited and regular talks at international conferences, and 4 international patents. His main research interests include the area of fiber optic transmission with particular interest in coherent optical systems, integrated optical transceivers, photonic subsystem for next-generation optical networks, and all-optical technologies. He has been involved in several European/National research projects and collaborations with private companies.

Philippe Velha received the Graduate degree in engineering and a Master of Science degree in integrated digital electronics from the École Centrale de Lyon, Lyon, France, in 2004, and the Ph.D. (Hons.) degree in silicon photonics from three different laboratories: Institut d'Optique, Laboratoire des Technologies de la Microelectronique, and SiNaPS from the CEA, Grenoble, France, in 2008. He is an established French Physicist whose expertise lies mainly in silicon photonics and nanofabrication. In this multidisciplinary environment, he designed, fabricated, and measured the first high-quality factor integrated microcavities known today as nanobeams. He became a Research Assistant with the University of Glasgow, Glasgow, U.K., in 2008. His research field spans from purely passive silicon photonics to more challenging topics such as light modulators, photodetectors, and integrated light sources on silicon. In June 2013, he joined the newly created Silicon Photonics Group at Scuola Superiore Sant'Anna, Pisa, Italy, where he is currently a Silicon Photonics Designer. His work has been published in several high-impact international peer-reviewed scientific journals. He is a coauthor, at the moment (2015), of more than 75 publications and a book, which is regularly cited as reference.

Michele Midrio received the M.S. and Ph.D. degrees in electronics and telecommunication engineering from the University of Padova, Padova, Italy, in 1991 and 1994, respectively. He was a Postdoctoral Research Fellow with the Fondazione Ugo Bordoni, Rome, Italy, for three years. He is currently a Professor of electromagnetics at the Dipartimento di Ingegneria Elettrica Gestionale e Meccanica, Università degli Studi di Udine, Udine, Italy. He has (co-)authored about 250 papers published in journals and conference proceedings. His current research interests include design of integrated optics, graphene, and antennas for both radio frequencies and optics.

Veronica Toccafondo received the M.Sc. degree in physics from the University of Pisa, Pisa, Italy, in 2005, and the Ph.D. degree in innovative technologies of ICT and robotics from the Scuola Superiore Sant'Anna, Pisa, Italy, in 2009. She is currently a permanent Researcher at the National Laboratory for Photonic Networks, Interuniversity National Consortium for Telecommunications, Pisa, Italy. She has been working on the design and characterization of integrated photonic structures, such as waveguide amplifiers and lasers, and integrated photonic biosensors for more than ten years. She joined the Advanced Packaging Laboratory of the institute in 2014 and her more recent research interests and expertise include the packaging of optoelectronic devices as well as the realization of prototypes based on them. She has worked in many national, regional, and EU projects as well as with industrial partners and is a (co-)author of more than 30 publications in international peer-reviewed journals and conference proceedings.

Stefano Faralli received the B.Sc. degree in physics from the University of Pisa, Pisa, Italy, in 2000, the M.Sc. degree in optical communications systems and networks from the Politecnico di Milano, Milan, Italy, in 2001, and the Ph.D. degree in telecommunications technology from Scuola Superiore Sant'Anna, Pisa, in 2006. In 2011, he was a Visiting Scholar with the University of California, Santa Barbara, CA, USA, working in the Optoelectronics Group. He is currently a Research and Process Engineer at the Scuola Superiore Sant'Anna. He is an author and coauthor of publications among patents and papers in peer-reviewed international journals and conference digests. His current research interests include integrated optics, silicon photonics, thin-film processing, distributed optical fiber sensors, Raman amplifiers, erbium-doped fiber, and waveguide amplifiers for wavelength-division multiplexing communication systems and networks.

Marco Romagnoli received the Graduate degree in physics from the Università di Roma "La Sapienza," Rome , Italy, in 1982. He is currently the Head of Advanced Technologies for Photonic Integration at the Interuniversity National Consortium for Telecommunications, Pisa, Italy, a contract Professor at Scuola Superiore Sant'Anna, Pisa, and the former Director in R&D Department. In 1983, he started his activity at IBM Research Center, San Jose, CA, USA. In 1984, he joined Fondazione Ugo Bordoni in the Optical Communications Department working on optical components and transmission systems. In 1998, he joined Pirelli, where he was the Director of Design and Characterization and a Chief Scientist in R&D Photonics. In October 2010, he joined PhotonIC Corporation, a Si-Photonics company, as the Director of Boston Operations and the Program Manager at the Massachusetts Institute of Technology for the development of an optically interconnected multiprocessor Si chip. He is an author of more than 190 journal papers and conference contributions and a coinventor in more than 40 patents. He is in the technical committee of the major conferences in photonics such as CLEO/QELS, CLEO Europe, ECOC, MNE, Group IV Photonics, and served as an expert Evaluator for EC in the 6th Framework Program. He has more than 35 years of experience in the research field, especially in the area of photonic technologies for TLC.

Luca Potì received the M.S. degree in electronics engineering from the University of Parma, Parma, Italy, in 1997. He is currently the Head of Research with the Interuniversity National Consortium for Telecommunications (CNIT) and the external collaborator for Scuola Superiore Sant'Anna, at the Institute of Communication, Information, and Perception Technologies, both located in Pisa, Italy. From 1998 to 2000, he was with the Optical Communications Laboratory at the University of Parma. Since 2001, he has been a Senior Researcher with CNIT at the Photonics Networks National Laboratory, Pisa. In 2002, he was a Visiting Researcher with the National Institute of Information and Communications Technology, Tokyo, Japan. He has published more than 200 international journal papers, conference papers, and patents. He was a Scientific Coordinator for the EU Project "Large optical bandwidth by amplifier systems based on tellurite fibers doped with rare earths." He was involved in several projects supported by the Italian Ministry of University and Research and the Ministry of Foreign Affairs. His research interests mainly include high capacity fiber optic transmission with particular interest in spectrally efficient coherent optical systems, photonic integration and photonic subsystem for next generation elastic optical networks.